BNL 19381

EUROPEAN ORGANIZATION FOR NUCLEAR RESEARCH

CERN/ISR-GS-TH/74-45

PRELIMINARY STUDY OF A CERN 400 GEV STORAGE-RING FACILITY

by

R.W. Chasman *, A.A. Garren **, K. Johnsen,
E. Keil, B.W. Montague and B.W. Zotter

MASTER

*) Visitor from Brookhaven National Laboratory, Upton, New York
**) Visitor from Lawrence Berkeley Laboratory, Berkeley, California

Geneva, Switzerland
September 10, 1974

PREFACE

This report is an updated version of CERN/ISR-GS/TH/74-34, "Options and Constraints in the Design of Future CERN Storage-Ring Facilities".

The main progress has been in the design of specific examples of experimental insertions, for which we can now give rather precise figures of physical layout and performance. This is only a first step. A continued programme of close collaboration between high-energy physicists and machine physicists will be necessary to ensure the evolution of insertion design leading to the best possible experimental facilities within the constraints of the machine itself.

1. INTRODUCTION

The purpose of this report is to summarize briefly the present status of our studies on large proton storage rings which have been under way for a few months. In particular we want to indicate possibilities, limitations and compromises of interaction region layout, to outline some examples for further discussion, and to disseminate quickly some of our ideas on future CERN colliding-beam facilities. Since the studies will continue, it will be necessary to revise the contents of this report from time to time.

Two models of a future CERN colliding-beam p-p project are at present under study, viz:

(A) 400 GeV rings using normal iron magnets

(B) 400 GeV rings using superconducting magnets

We have also given some thought to a superconducting conversion of the ISR in the existing tunnel [1]. At field levels achieved in superconducting magnets at present of about 4 T, and with reasonable lengths of intersection regions, the maximum energy in this machine would be about 100 GeV or a little higher. This energy seems rather low at CERN where 28 GeV storage rings already exist, and where a 400 GeV injector synchrotron, the SPS, will soon become available.

The maximum energy of the storage rings is chosen within the energy range of the SPS, because it permits the energy stacking method to be used, as in the ISR, and avoids the acceleration of the stacked beam to a higher energy. The energy reached with this assumption, 400 GeV, appears to be high enough that a detailed examination of accelerating storage rings need not be undertaken at this moment.

Model (A) has been our main preoccupation during the last few months, chiefly because it became clear last year, as a result of work at BNL, that the performance limitations of large-circumference storage rings had not been adequately understood. Now, however, we are confident that storage rings with normal magnets and good performance can actually be built. In order to achieve a luminosity of 10^{33} $cm^{-2}s^{-1}$, a minimum current of 5 A is needed. The resulting problem of dumping a beam with that stored energy must be solved. First indications from an engineering study are that this can be done with an external beam dump.

Model (B) has so far been looked at only superficially though we are following closely the considerable effort in other laboratories, and in particular at BNL. We shall turn our attention in this direction much more in the coming months, since superconducting machines offer better performance prospects than normal ones.

Much of the thought given to the problems of a normal-magnet design is applicable to a superconducting machine. Furthermore, the constraints imposed by rings of large circumference on the CERN site highlight the problems of designing interaction regions. We are therefore using model (A) in this report as a "guinea pig" for resolving the conflicting requirements of machine design and physics experiments, with confidence that the main conclusions to be drawn from this exercise will be relevant to superconducting-magnet machines as well.

2. MACHINE LATTICE

The circumference of the machine is made up by two contributions: the normal lattice which occupies the greater part, and the colliding beam insertions which occupy the rest. Consequently, the largest contributions to single beam space charge phenomena come from the normal lattice, while the beam-beam space charge (and high-energy physics) phenomena only occur in the insertions. It is therefore convenient for a preliminary analysis to consider these two contributions separately.

Experience with the ISR has shown that the Q-values have to be controlled with rather high precision if one wants to avoid enhanced beam decay rates due to non-linear resonances in the stacked beam. This imposes tight tolerances on the power supplies, on the changes of the Q-values by space charge phenomena, and on the range of Q-values present within the beam. In particular, the design of the machine must ensure that the image-dominated incoherent tune shift is below the limit imposed, and that the circulating beam is transversely stabilized by the small Q-spread available. It turns out that these requirements can be met by choosing a sufficiently large aperture over most of the circumference of the machine. In contrast to conventional accelerators, the aperture of a large-radius storage ring is not determined by the beam size, closed orbit distortions, beam gymnastics and the like, but rather by the requirement that the vacuum chamber walls and magnet polepieces be far enough from the beam that their eletromagnetic effect on it can be handled. At the same time a large machine aperture helps to avoid vacuum problems due to beam-induced gas desorption.

A formalism which takes these space charge phenomena into account and leads to the physical parameters of a machine has been described elsewhere [2]. For the machine which is used as a basis in this report, we have chosen the aperture radius such that the incoherent Q-shift and the Q-spread both are smaller than 0.02. The machine parameters arrived at in this manner are shown in Table I. The layout of the lattice and the betatron and dispersion functions are shown in Fig. 1.

3. HORIZONTAL OR VERTICAL ARRANGEMENT OF RINGS AND CROSSINGS?

The two rings may either be built side by side, with horizontal crossings as in the ISR, or one ring may be put above the other, with vertical beam crossings. In a third arrangement, presently adopted for ISABELLE [3], the rings are arranged vertically while the crossings are horizontal. Closely related to the plane of crossing is the distance between the beams in the two rings. If the rings are installed vertically the best separation would be about 1 m, while for the horizontal arrangement a distance of about 2.5 m would be most convenient. This allows the two rings to be installed along the inner and outer tunnel walls with a common access space between them.

There now seem to be no compelling beam dynamics arguments for one choice or the other, which may hence be made on the basis of practical considerations such as tunnel size, length and layout of various types of intersections, and convenience for experiments at the crossing points.

For the purposes of this report we have chosen the horizontal arrangement of the magnets and a separation of 2.5 m. We have also designed some intersection regions for vertically separated rings with 1 m distance. A comparison between these designs shows that a small separation is more favourable for some types of intersection regions while the opposite holds for other types. This applies both to horizontal and vertical stacking of the two rings. Further studies of these alternatives will be undertaken.

4. TYPES OF INTERACTION REGION

For given energy and stacked current, the maximum design luminosity of an interaction region is limited mainly by two factors, viz. the non-linear electromagnetic beam-beam interaction, and the maximum acceptable values of betatron function in the neighbouring quadrupoles. The first is fundamental but not well quantified, and the second is limited by chromaticity and tolerances. Both factors lead to a situation in which a compromise between luminosity and field-free length around the interaction region must be made.

One is therefore led to consider a machine with two or more types of interaction region, each designed to be suitable for a particular class of experiment. We have so far considered three types of interaction region, a high-luminosity low-β region, a general-purpose interaction region with plenty of unencumbered space, and a high-β region with special optics for measurement of very small scattering angles. Examples of these interaction regions are outlined in subsequent sections and their parameters are summarised in Table II.

The luminosity $\mathcal{L}$ and beam-beam Q-shift ΔQ are given with sufficient accuracy for the general-purpose and high-β crossings (but not for the high-luminosity insertion) by the approximate formulae:

$$\mathcal{L} = \frac{2c\ n^2}{\alpha} \sqrt{\frac{\gamma}{\beta_0\ \epsilon}}$$

$$\Delta Q = \frac{\sqrt{2}\ r_0\ \beta_0}{c\ n\ \gamma} \cdot \mathcal{L}$$

where n = number line density of protons

β_0 = beta-function at crossing point in plane perpendicular to intersection plane

ϵ = normalised emittance

γ = energy factor

r_0 = classical radius of proton

For the high-luminosity region, the parameters are chosen to reach the assumed beam-beam limit (ΔQ = 0.005). The general-purpose and high-β insertions have appreciably smaller Q-shifts, however, as they were designed to provide certain beam optical properties and free space for experimental equipment, rather than maximum luminosity.

In discussing lengths of interaction regions it is necessary to distinguish between the total length of the insertion and the length of field-free space around the interaction volume unencumbered by machine elements. In some configurations there is useful space available for detectors outside the vicinity of the interaction volume, in the high-β insertion for example, where the beam transport properties of the insertion have been specially contrived to help in the design of the detector arrangement for small angles.

4.1. High-Luminosity Regions

This example gives a luminosity of 1.2×10^{33} $cm^{-2}s^{-1}$ for stacks of 5 A and a field-free space of $\pm$ 10 m about the centre. This would be changed if engineering work on the beam-dumping problem yielded a different maximum current, or if the beam-beam limit were to correspond to a linear ΔQ different from the 0.005 we assume at present.

The layout of this region is shown in Fig. 2 and the betatron functions and dispersion in Fig. 3. The use of superconducting separating magnets, of 3.7 T say, would permit a field-free length of about ± 15 m.

4.2. General-Purpose Regions

The present model has a crossing angle of 19.4 milliradians, a calculated luminosity (5 A stack) of 1.6×10^{31} $cm^{-2}s^{-1}$ and 80 m of unobstructed space each side of the interaction region. The layout is shown in Fig. 4 and the betatron functions and dispersion in Fig. 5. The crossing angle was chosen to be the same as that of the high-β region, in order to standardise the geometry. A reduction in crossing angle to increase the luminosity would be possible only by the introduction of separating magnets into the otherwise unencumbered space of ± 80 m around the crossing point.

4.3. High-β Regions

Here the beam optics have been arranged to achieve spatial separation of particles at very small angles to the beam without excessively long drift spaces. High β-values of 400 m in both planes permit scattering angles down to $\sim$ 20 μrad to be measured by devices similar to Roman pots. These high-β regions have a similar total length and crossing angle to the general-purpose regions. Although there are quadrupoles near the crossing point, a large fraction of the total length of the region is free for installing detectors. The calculated luminosity for 5 A stacks is 3.3×10^{30} $cm^{-2}s^{-1}$. Fig. 6 shows the arrangement, and Fig. 7 and 8 the betatron functions and dispersion. The measuring error for small scattering angles is minimized by having 90° phase advance from the intersection and an α_p cross-over at the detector.

5. NUMBER OF INSERTIONS

The number of insertions is determined by the scale and scope of the physics programme which the storage rings are supposed to support. In addition, special insertions will be required for injection and beam dumping. It seems likely that a minimum of six interaction regions will be required for physics experimentation, especially if more than one type is necessary, as seems likely.

A racetrack configuration with grouped interaction regions has been chosen. Any machine with 6 intersection regions of 3 types has the low superperiodicity of two. This choice brings two types of problems, both tractable in our opinion. Firstly, it makes the machine rather sensitive to perturbations arising both from structure imperfections and from beam-beam effects. Some care is needed to avoid further asymmetries which could produce appreciable disturbances with a superperiodicity of unity. All intersections are strong potential sources of perturbations and must be arranged symmetrically between the two groups of interaction regions. Compared with CERN/ISR-GS/TH/74-34, the present example has some reverse bending and sections of machine lattice, introduced to ease the matching.

The second problem is to prevent the large flux of particles scattered at small angles in a high-luminosity region from generating background in neighbouring interaction regions. The sections of normal lattice between intersections will help to minimize such background.

The configuration of the crossing regions must be chosen to avoid systematic effects of unit periodicity, either from the structure or from the beam-beam forces.

Taking into account the various constraints of symmetry, topology, injection and beam dumping, a reasonable example with six interaction regions would include two with high luminosity. The remaining four, could either all be general-purpose, or one could have two g-p and two high-β.

In the model at present considered, the injection and dumping insertions would be in the arcs of the racetrack configuration. Symmetry requires that the beams cross in these regions though they might be separated to avoid unnecessary beam-beam effects. The injection arrangement from the SPS will have to be studied bearing in mind the siting of the storage rings, the transfer tunnels and the ejection equipment already provided in the SPS.

The beams move outwards in the high-luminosity interaction regions and in the injection/dumping insertions, and move inwards in the other four interaction regions. This is a favourable arrangement for external dumping and for injection. With the change in topology of the experimental insertions, compared to the previous report, the crossing direction is no longer important to them.

REFERENCES

1) D.A. Swenson; CERN/ISR-GS/74-35 (1974)

2) E. Keil; CERN/ISR-TH/74-22 (1974)

3) H. Hahn and M. Plotkin, eds.; BNL 18891 (1974)

Table I: Parameter list for large storage rings

Maximum momentum	400 GeV/c
Maximum bending field	1.8 T
Circumference / 2π	1268 m
Average radius of normal lattice	983 m
Stored current	5 A
Stored energy in beam	52.6 MJ
Maximum single beam tune shift	0.02
Maximum tune spread	0.02
Vacuum chamber aperture radius	30 mm
Betatron wavenumber	≈ 35.25
Period length	57.2 m
Quadrupole length	3.3 m
Bending magnet length	7.2 m
Number of periods	108

Table II: Performance estimates for the 3 model insertions

	Low Beta	High Beta	General Purpose
Luminosity ($cm^{-2}s^{-1}$)	1.2×10^{33}	3.3×10^{30}	1.6×10^{31}
Beam-beam Q-shift	4.8×10^{-3}	2.2×10^{-3}	4.8×10^{-4}
β_v (m)	1.3	400	18
β_h (m)	5.0	400	58
Crossing angle (mrad)	0.9	19.4	19.4
Field-free half-length (m)	10	15	80

The above data are for:

Stacked current	I = 5 A
Normalised emittance	$\epsilon = 30\pi \times 10^{-6}$ rad m (both planes)
Energy	400 GeV ($\gamma = 426.3$)

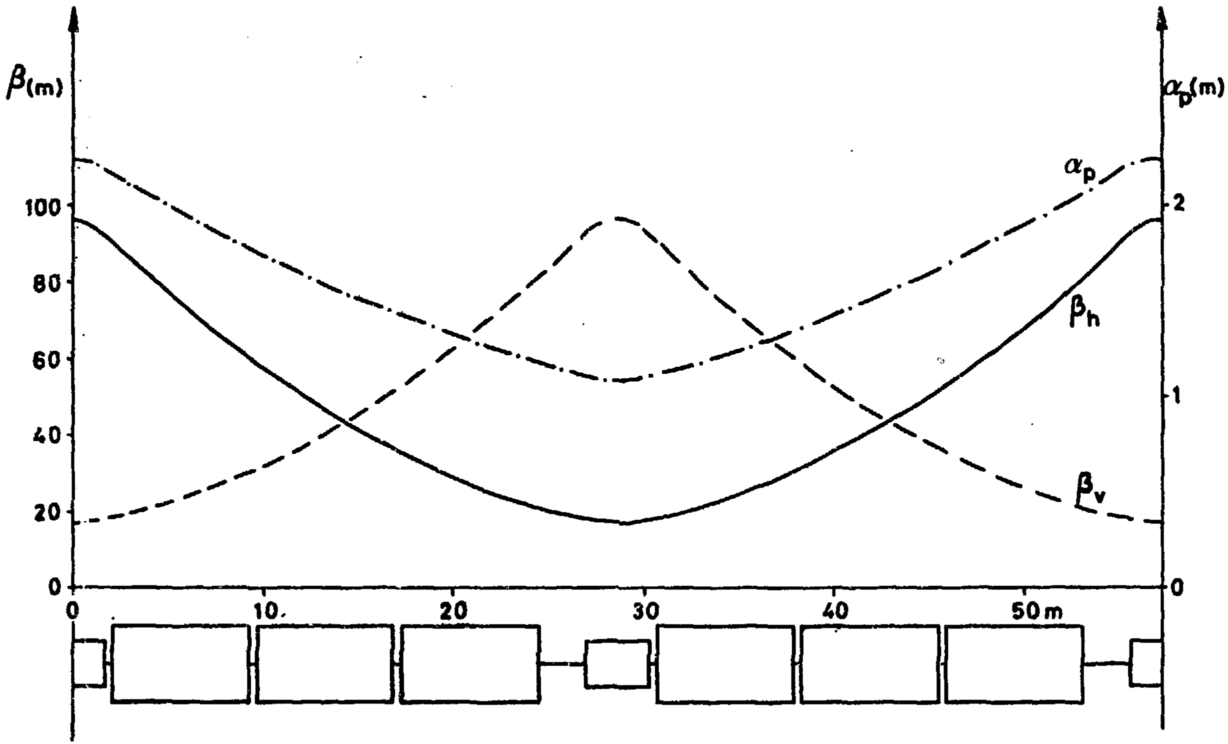

Fig. 1

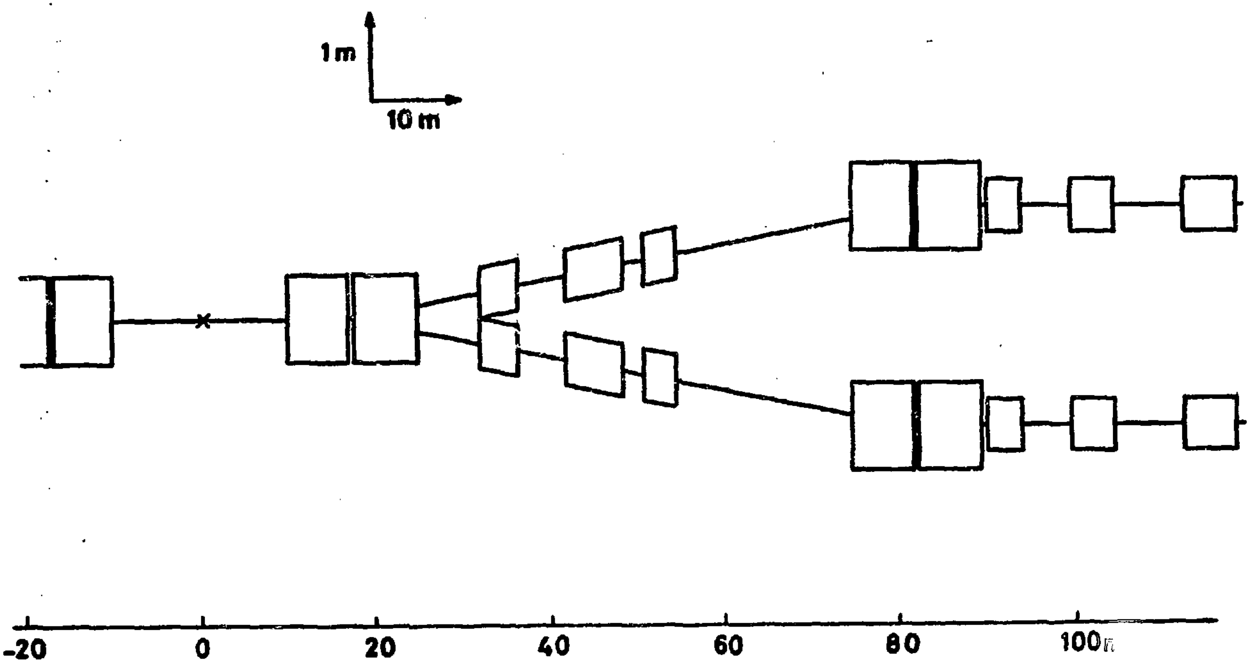

Fig. 2

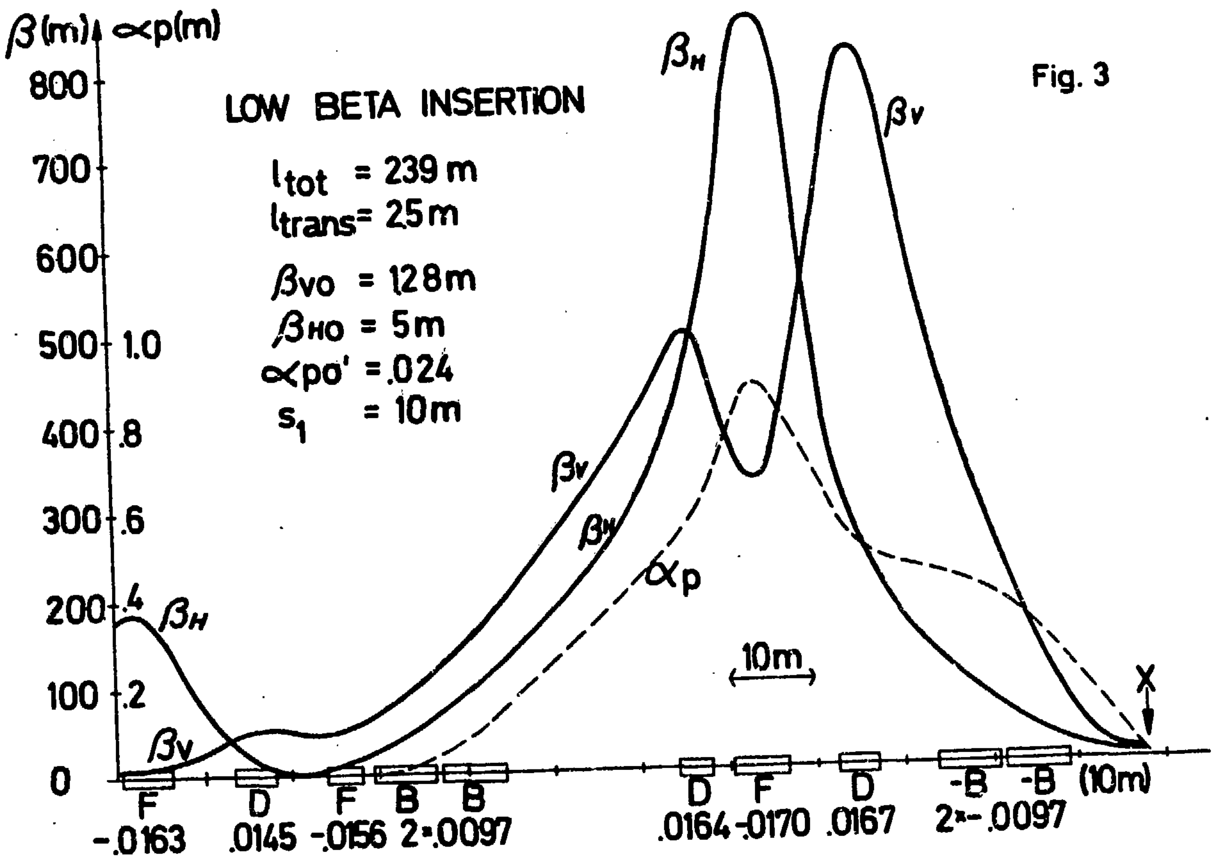
β(m) ∝p(m)
800
700
600
500 1.0
400 .8
300 .6
200 .4
100 .2
0
LOW BETA INSERTION
l_tot = 239 m
l_trans = 25 m
βvo = 128 m
βHO = 5 m
∝po' = .024
s1 = 10 m
βH
βV
βV
βH
αp
βH
βV
10m
X
F
-.0163
D
.0145
F
-.0156
B B
2×.0097
D
.0164
F
-.0170
D
.0167
-B -B
2×-.0097
(10m)
Fig. 3

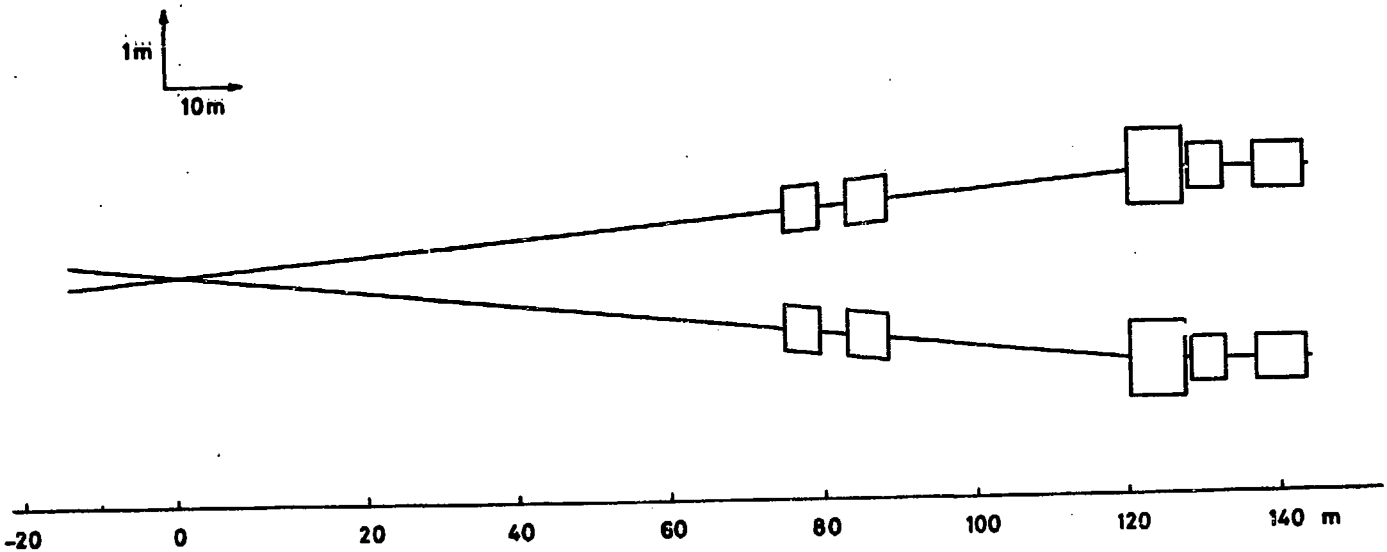

Fig. 4

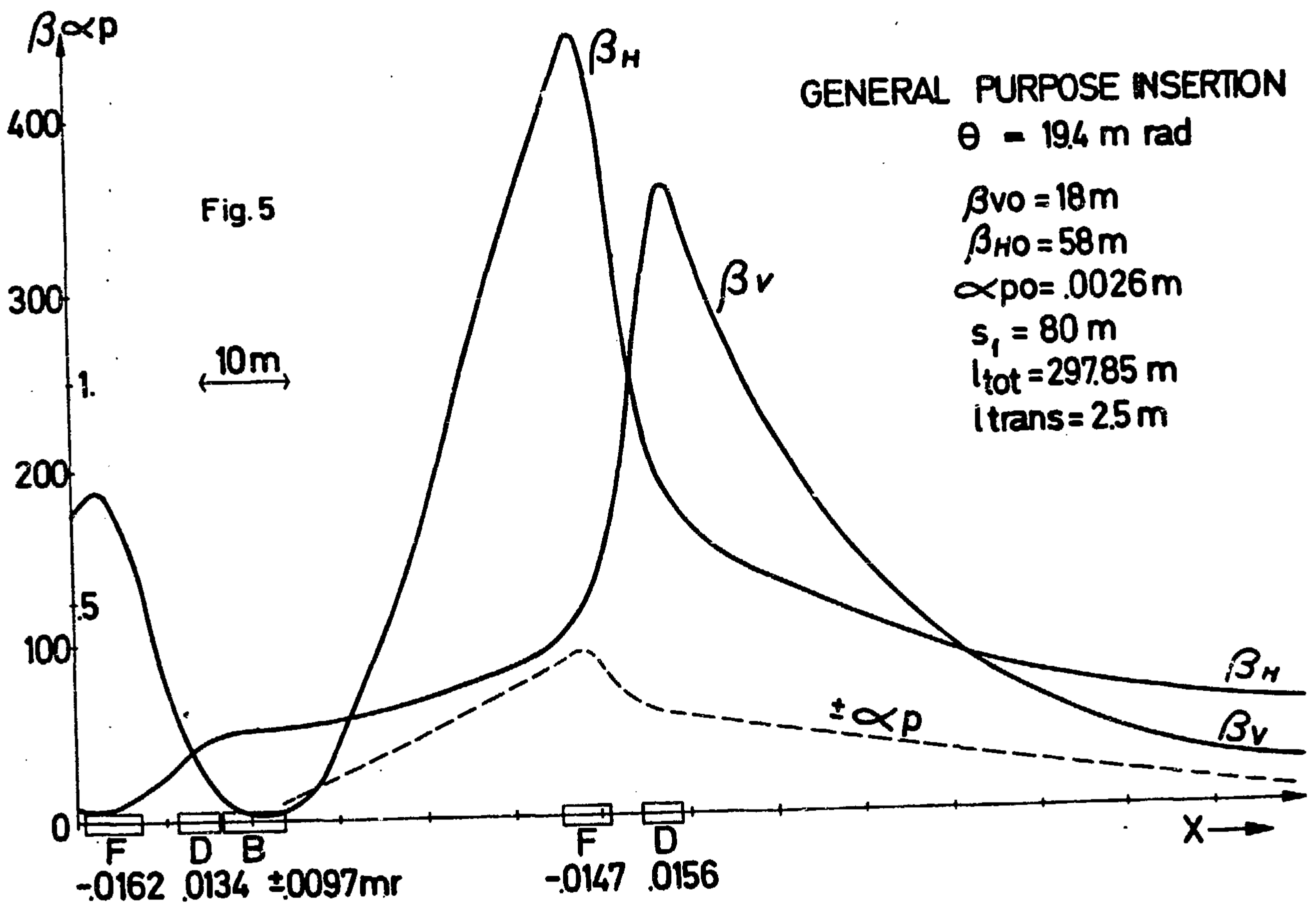

β αp
400
300
200
100
0
1.
.5
Fig. 5
10m
βH
βV
±αp
X
F
D
B
-.0162
.0134
±.0097mr
F
D
-.0147
.0156
GENERAL PURPOSE INSERTION
θ = 19.4 m rad
βvo = 18 m
βHO = 58 m
αpo = .0026 m
s1 = 80 m
ltot = 297.85 m
l trans = 2.5 m

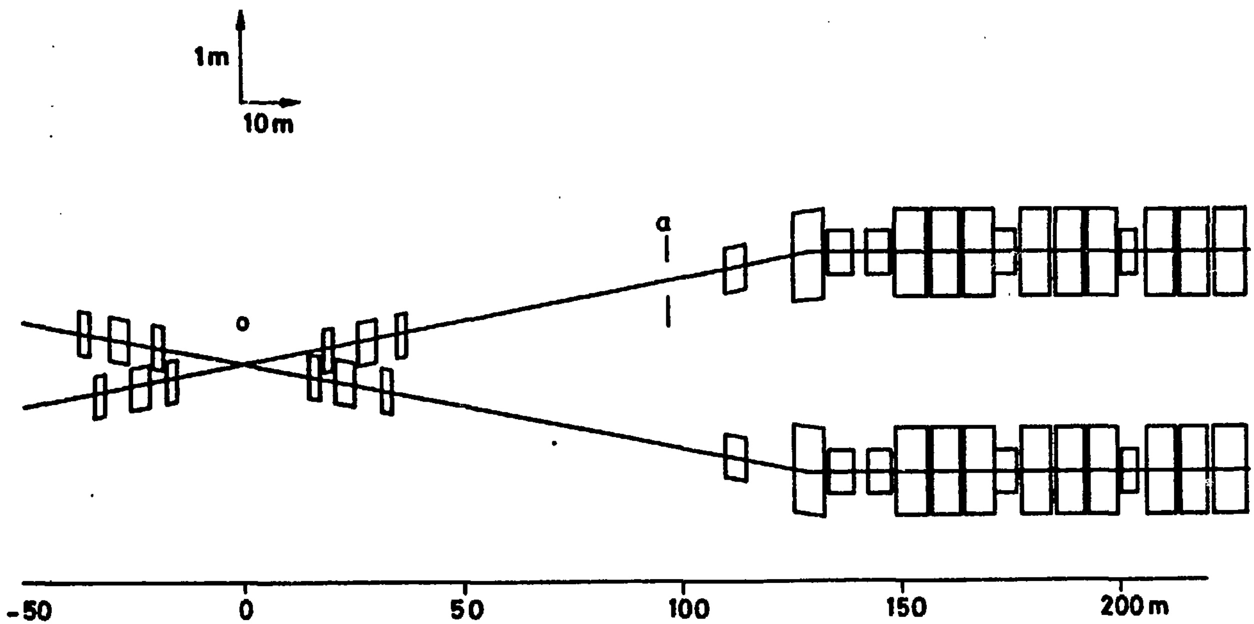

Fig. 6

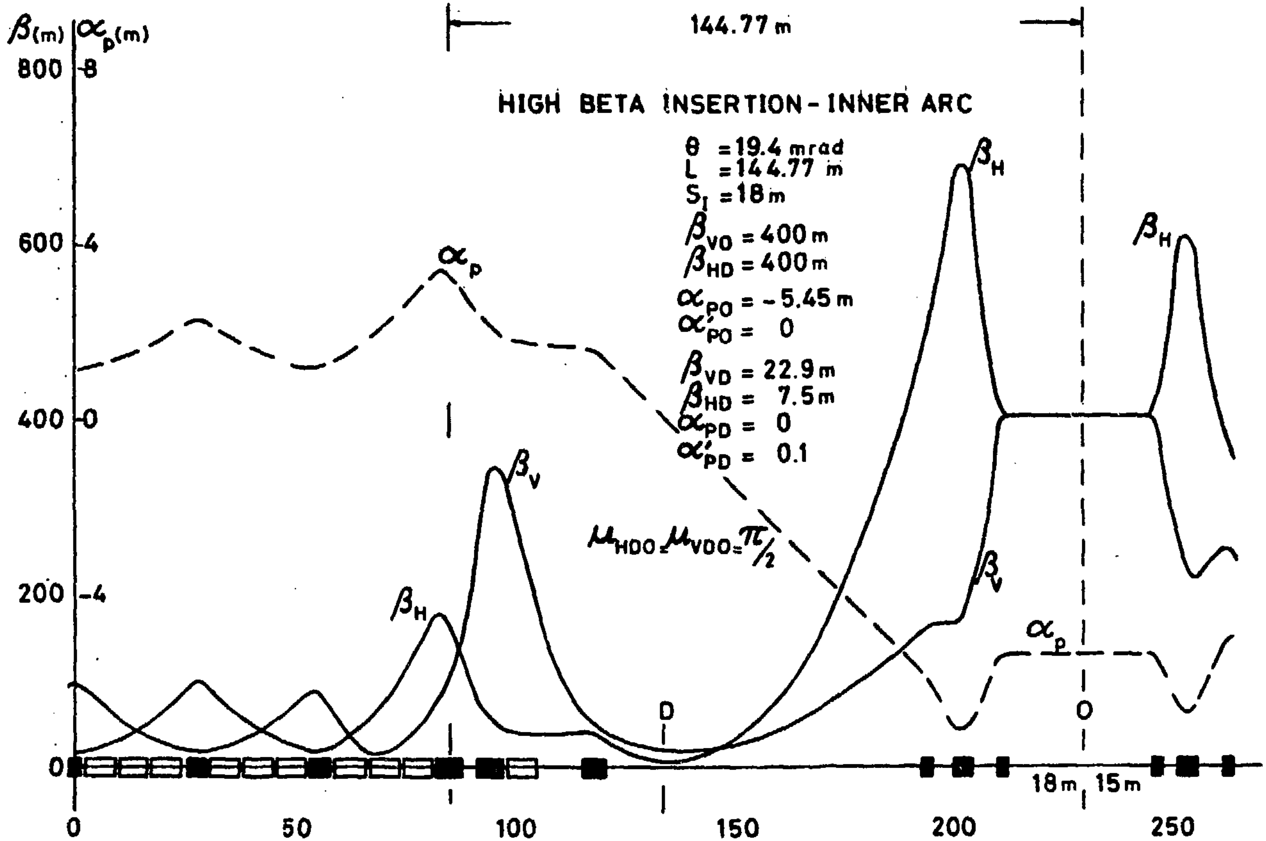

β(m)
αp(m)
800
600
400
200
0
8
4
0
-4
144.77 m
HIGH BETA INSERTION - INNER ARC
θ = 19.4 mrad
L = 144.77 m
SI = 18 m
βVO = 400 m
βHO = 400 m
αPO = -5.45 m
α'PO = 0
βVD = 22.9 m
βHD = 7.5 m
αPD = 0
α'PD = 0.1
μHDO = μVDO = π/2
αp
βV
βH
D
O
18 m
15 m
0
50
100
150
200
250

Fig. 7

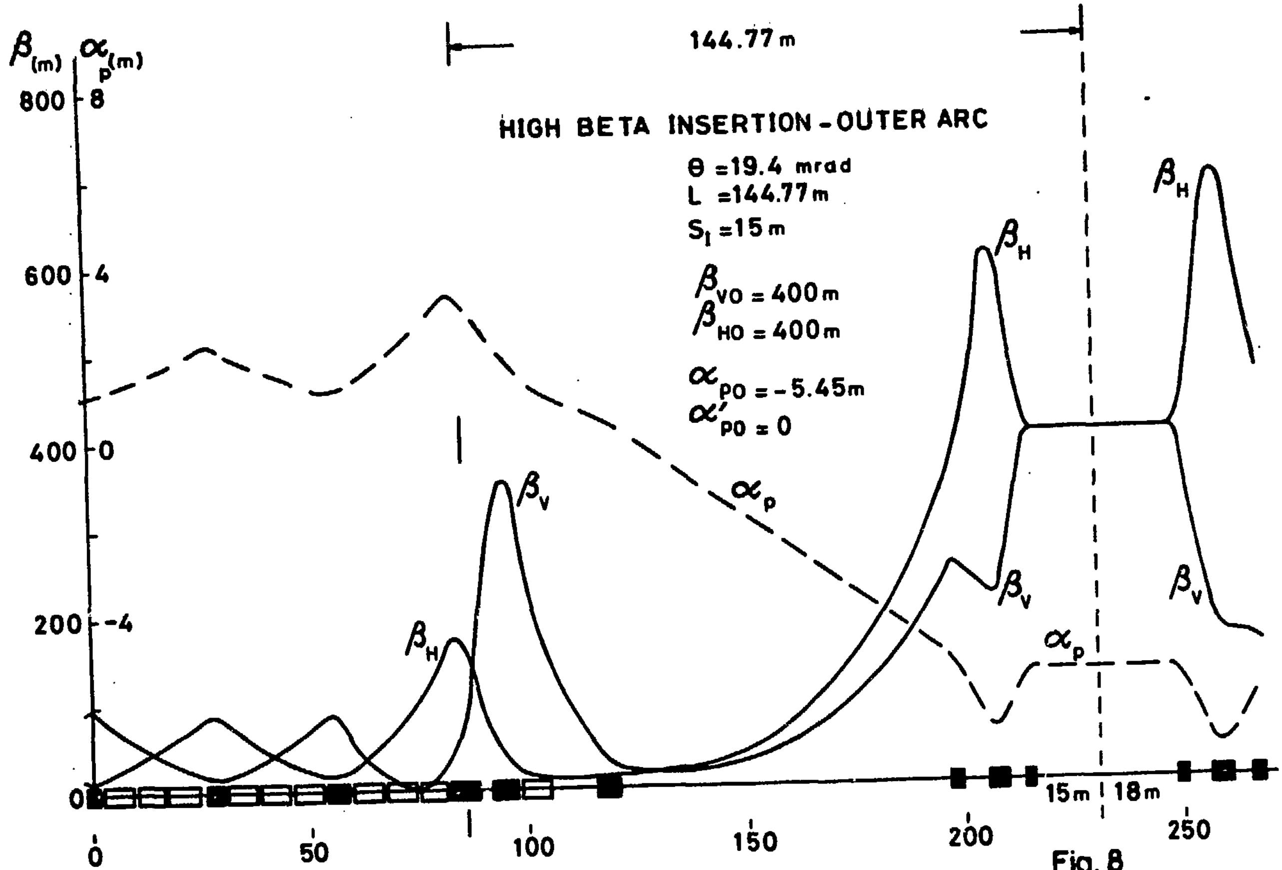
144.77 m
HIGH BETA INSERTION - OUTER ARC
θ = 19.4 mrad
L = 144.77 m
S_l = 15 m
β_VO = 400 m
β_HO = 400 m
α_PO = -5.45 m
α'_PO = 0
β(m)
α_p(m)
800
600
400
200
0
8
4
0
-4
β_H
β_V
α_p
15 m
18 m
0
50
100
150
200
250

Fig. 8